Peter Bruns* and Jens Twiefel

Influences of Non-axial Process Loads on the Transducer and the Associated Mounting in Ultrasonic Machining

Abstract: An analysis method allowing investigations of load influences on ultrasonic transducer oscillations is developed and presented. The focus here is on transducers utilized in ultrasonic-assisted machining due to the high process loads occurring. These loads can affect the operational vibration by exciting bending or torsion modes. However, the explicit impact on the process has yet to be determined. Hereby, conclusions about each oscillation mode effecting the operational vibration separately would be desirable. To achieve this, the eigenmodes being excited in dependence of the load have to be determined. Though the question remains of how big the respective influence on the operational vibration is. In the contribution at hand both questions will be answered by means of a modal transformation-based analysis that is illustrated by an explicit example. It is shown that a defined modal force permits determining the excited modes and the explicit share of the applied load coupling into the particular mode, respectively. In addition, the qualitative impact of each eigenmode on the resulting vibration can be evaluated by means of the magnitude of the modal equation's particular solution. The developed analysis is applied on process and mounting loads. Therefore, different load setups are investigated in dependence of the force direction and the application point, thus leading to the conclusion that the presented analysis method is versatile usable, trustable and efficient.

Keywords: ultrasonic actuators, longitudinal transducers, process loads

DOI 10.1515/ehs-2014-0022

***Corresponding author: Peter Bruns,** Institute of Dynamics and Vibration Research, Leibniz Universität Hannover, Hannover, Germany, E-mail: bruns@ids.uni-hannover.de
Jens Twiefel, Institute of Dynamics and Vibration Research, Leibniz Universität Hannover, Hannover, Germany, E-mail: twiefel@ids.uni-hannover.de

Introduction

Superimposing ultrasonic vibrations to actual machining processes on one hand makes machining of intractable materials possible (Babitsky et al. 2003) and offers various advantages on the other hand. The most important advantages here are the reduction in friction and thus process forces (Littmann, Storck, and Wallaschek 2001; Heisel et al. 2011) as well as an improved surface quality (Babitsky et al. 2003). Due to the associated benefits superimposing ultrasonic vibration to more and more processes, such as cutting, turning or grinding, is attempted and ultrasonic-assisted machining becomes established in industry. Thus, dimensioning and designing of the ultrasonic source and its coupling is important in the machining development. The focus is on the improvement of the system characteristics such as efficiency and overall costs. Through the integration of the ultrasonic source though, its vibration isolation to the environment becomes important as well. Typically, this is realized utilizing appropriate mountings, which are usually designed similar to the proposals in Rozenberg et al. (1964) or resulting approaches (e.g. Rozenberg 1969; Crispi, Maling, and Rzant 1972; Zhang et al. 2013).

However, the mounting of ultrasonic transducers has not been covered sufficiently by researchers and engineers. Especially, the used assumption of free vibration of the transducer is not valid in many setups for ultrasonic-assisted machining processes. Even excitation of bending or torsion modes is possible due to the occurring process loads. Promising potentials for improvement of the mounting and respectively the overall system behavior, this also means that the process load influence on the transducer oscillation ought to be investigated more closely. With conclusions about each oscillation mode effecting the operational vibration separately being desirable, the question needs to be answered:

1. Which oscillation modes can be excited in dependence of the process load?

However, determining the eigenmodes being excited doesn't allow conclusions about the explicit impact on the process itself. Since each oscillation mode makes a specific contribution to the resulting oscillation of the transducer a second question needs to be answered:

2. How is the operational vibration affected by the determined oscillation modes?

Both questions will be answered by means of a modal transformation-based analysis method developed and presented in the following. The entire method here stands out due to particular simplicity as well as short computational time. These benefits are a result of the innovative analysis that is carried out on the modal transformation results directly. Whereas excitation magnitude and impact of disturbing modes for a certain frequency range can be determined for each single oscillation mode separately, as required.

Modeling Method and Evaluation

Examined Example

The developed analysis method is illustrated by means of a representative example. The selected transducer (length 228 mm, min. diameter 18 mm, max. diameter 52 mm) illustrated in Figure 1 originates from an application for machining of stone [8]. Superimposing ultrasonic vibrations to the actual milling process leads to a significant reduction of process forces while working on the brittle and intractable material. Thus a considerably longer tool life can be achieved, which is very important because of the extremely expensive tools utilized (Weaver, Timoshenko, and Young 1990).

However, in the milling process at hand forces perpendicular to the transducer's vibration direction occur due to the feed motion. Thus the operating mode is affected with the explicit effects yet to be determined. In order to achieve this, the transducer has to be modeled in the form of a finite element (FE) model first, whereas the process load is not considered. With the analyzed transducer being modeled in an FE program not only determination of eigenmodes (an extract of the modal analysis is given in Table 1) but also a direct export of the mass matrix M and stiffness matrix C is possible. These matrices can be put directly in the differential equation of motion which is required for further steps.

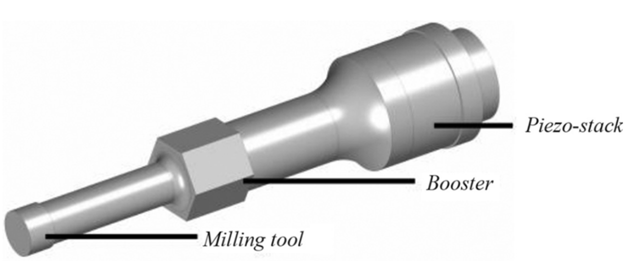

Figure 1: FE model of examined transducer with bonded contacts between components.

Table 1: Extract from list of oscillation modes.

Mode no.	Frequency (Hz)	Mode type
16	19,029	Bending
17	19,129	Bending
18	21,016	Longitudinal (operat. mode)
19	26,286	Torsion
20	27,315	Bending

It should yet be mentioned here that the longitudinal mode no. 18 is the operational mode, due to the fact that the overall system is explicitly designed for this mode.

Equation of Motion

The presented method requires the differential equation of motion for the transducer investigated. Assuming the system to be linear, time invariant and vibration capable we obtain according to (Weaver, Timoshenko, and Young 1990):

$$\underline{M}\,\ddot{\underline{x}} + \underline{D}\,\dot{\underline{x}} + \underline{C}\,\underline{x} = \underline{F}(t) \qquad [1]$$

whereas mass M and stiffness matrix C gained from the FE model are of $N \times N$ dimension with N being the number of degrees of freedom (DOF). Assuming that only frequency independent structural damping occurs, allows replacing the matrix D by an $N \times N$ diagonal matrix. Thus the calculations are simplified, with future extension of other damping modeling being still possible.

The examined load is approximated in form of a harmonic excitation $\underline{F}(t)$. In the investigations carried out only harmonic forces exerting at one of the nodes on the tool's front face (cf. Figure 2, left) are considered. Furthermore, the influence of a non-axial load is examined by making the occurring force angle dependent as shown in Figure 2 (right). Thus the amplitude of the vector $\underline{F}(t)$ retains the entries

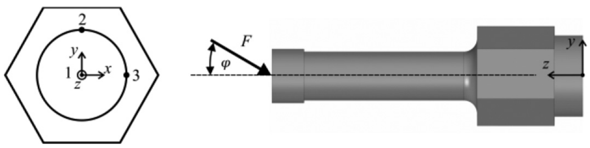

Figure 2: Node numbering on tool's front face and schematic drawing of load angle.

$$\underline{\hat{F}} = \begin{bmatrix} \vdots \\ \hat{F}_{i,x} \\ \hat{F}_{i,y} \\ \hat{F}_{i,z} \\ \vdots \end{bmatrix} = \begin{bmatrix} \vdots \\ 0 \\ F\sin(\varphi) \\ F\cos(\varphi) \\ \vdots \end{bmatrix} \qquad [2]$$

at the respective positions belonging to the examined node. The remaining entries have to be filled with zeros. Solving the equation of motion (eq. [1]) with well-known methods (Weaver, Timoshenko, and Young 1990) provides, for example, the system response or the frequency response. An extract of the latter for the examined transducer is given in Figure 3 for the sake of completeness. However, more information can be obtained by investigating the approach through modal transformation in detail.

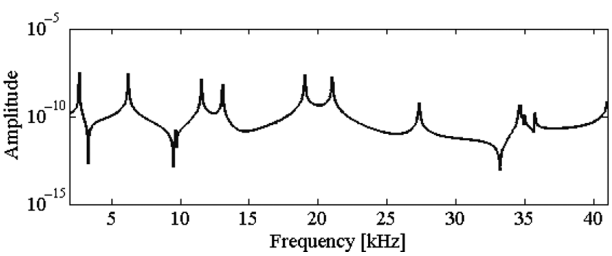

Figure 3: Frequency response for z-direction with harmonic force at the center of tool's front face (node 1).

Modal Transformation

In accordance with (Weaver, Timoshenko, and Young 1990), applying the solution approach

$$\underline{x} = \underline{\hat{x}}\, e^{\lambda t} \qquad [3]$$

leads to the characteristic equation

$$\det\left(-\underline{M}\,\lambda^2 + \underline{D}\,\lambda + \underline{C}\right)\underline{\hat{x}} = \underline{0} \qquad [4]$$

with the non-trivial solution of eq. [4] delivering the eigenvalues λ_n. Inserting these values into the N-dimensional linear equation system allows the identification of the respective independent eigenvectors, which can be used to determine the modal mass m_n:

$$\underline{\hat{x}}_k^T\,\underline{M}\,\underline{\hat{x}}_n = \begin{cases} m_n & \text{for } k = n \\ 0 & \text{for } k \neq n \end{cases} \qquad [5]$$

and modal stiffness k_n, respectively. Now, in turn, the eigenvectors can be standardized to the modal mass:

$$\underline{\hat{u}}_n = \frac{1}{\sqrt{m_n}}\,\underline{\hat{x}}_n \qquad [6]$$

and combined into the modal matrix Φ:

$$\underline{\Phi} = \begin{bmatrix} \vdots & & \vdots \\ \underline{\hat{u}}_1 & \cdots & \underline{\hat{u}}_N \\ \vdots & & \vdots \end{bmatrix} \qquad [7]$$

with the columns indicating the eigenmode and the rows indicating the respective DOF movement. Now eq. [1] can be transferred into the modal space by introducing the coordinate transformation

$$\underline{x} = \underline{\Phi}\,\underline{y} \qquad [8]$$

and multiplying with the transposed modal matrix:

$$\underline{\Phi}^T\underline{M}\,\underline{\Phi}\,\underline{\ddot{y}} + \underline{\Phi}^T\underline{D}\,\underline{\Phi}\,\underline{\dot{y}} + \underline{\Phi}^T\underline{C}\,\underline{\Phi}\,\underline{y} = \underline{\Phi}^T\underline{F}(t) \qquad [9]$$

Due to orthogonality relations the obtained system of differential equations is decoupled and corresponds to N systems with only one DOF (Weaver, Timoshenko, and Young 1990). Above steps thus allow an analysis of each single oscillation mode occurring separately without requiring further complex calculation steps.

Evaluation of Process Loads

The obtained system of differential equations (eq. [9]) offers various evaluation options. Looking first only at the equation's right-hand side

$$\underline{q}(t) = \underline{\Phi}\,\underline{F}(t) \qquad [10]$$

observations about force coupling for each vibrational mode in dependence of load conditions can be made. Specifically, this means that the modal force vector $\underline{q}(t)$ is filled with scalar values, which describe the coupling of the applied force into the particular eigenmode. A high modal force value here means that the force applied on the real system has a strong effect on the respective eigenmode.

Analyzing the modal force vector relating to the example at hand (cf. Figure 2) leads to the bar diagrams given in Figures 4–6, whereas the first 30 eigenmodes

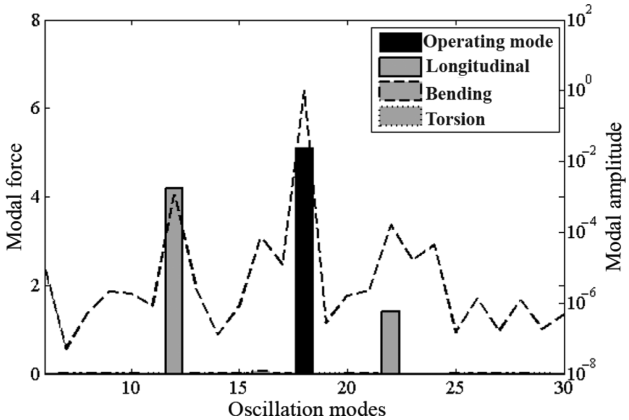

Figure 4: Modal force and modal amplitude at operational frequency (dashed line) for excitation at node 1 with $\varphi = 0°$.

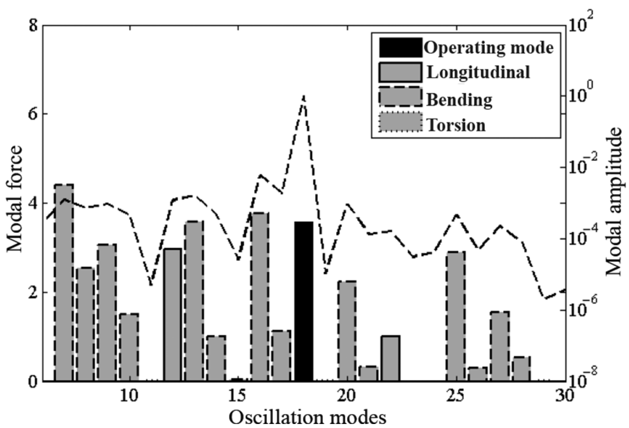

Figure 5: Modal force and modal amplitude at operational frequency (dashed line) for excitation at node 1 with $\varphi = 45°$.

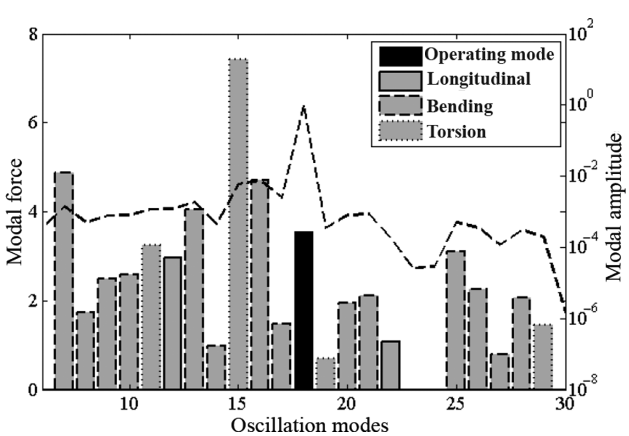

Figure 6: Modal force and modal amplitude at operational frequency (dashed line) for excitation at node 3 with $\varphi = 45°$.

except for the rigid body modes are shown. As might be expected, the applied harmonic force almost entirely couples into the longitudinal modes for an axial force ($\varphi = 0°$) at node 1. Increasing the load angle φ obviously leads to a coupling into bending modes as well. With changing the force application position in x-axis direction (node 3) even a coupling into torsion modes can be observed, as shown in Figure 6.

Thus being able to answer the first question posed above by means of the defined modal force, however, it does not yet allow any conclusion regarding the explicit impact on the operational vibration. To achieve this further transformation of eq. [9] is necessary.

Since the system of differential equations is transferred into the modal space, the particular solution for each DOF can be written as

$$y_n(t) = \frac{1}{m_n} \frac{1}{-\Omega^2 + (1 + i\, d)\omega_n^2} \hat{F}_n e^{i\Omega t} \quad [11]$$

with consideration of damping being assumed as structural damping d and the eigenfrequencies ω_n

$$\omega_n = \sqrt{\frac{k_n}{m_n}} \quad [12]$$

Defining the magnitude of $y_n(t)$ as the modal amplitude, it is a measure of the oscillation mode excitation at a particular frequency Ω. Evaluating the modal amplitude thus shows the particular mode's share of the entire real solution at a particular node.

For the considered example the maximum values of the modal amplitude for each eigenform in a frequency band of ± 50 Hz around the operating frequency (cf. Table 1) are shown in Figures 4–6 in the form of dashed lines. Here the values are normalized to the operating mode's modal amplitude with the y-axis scaled in a logarithmic format. Considering the force application position at node 1, it becomes apparent that the impacts of bending and torsion modes are about three orders of magnitude smaller than the operating mode. Hence the impact on the operational vibration can be considered negligible. Changing the force application position to node 4 though increases the modal amplitude of the torsion mode (no. 15) to approx. 10% of the operating mode's value. Thus the real operational vibration might be noticeably affected under the conditions described. However, the above posed second question, considering the impact of certain eigenmodes on the operational vibration, can be answered by means of the defined modal amplitude.

Evaluation of Mounting Loads

Exchanging the process load with a mounting load allows investigation of the influences on the oscillation caused by the mounting. For this purpose the load is approximated as harmonic forces that are applied near an oscillation node of mode no. 18, as shown in Figure 7. Thus it is only necessary to adjust the vector $\underline{F}(t)$. Further calculations can be carried out as described above. Again leading to the respective bar diagrams, direct conclusions about the transducer mounting become apparent.

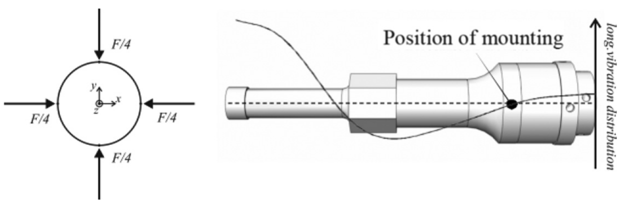

Figure 7: Schematic drawing of applied radial mounting load and curve of longitudinal oscillation mode no. 18.

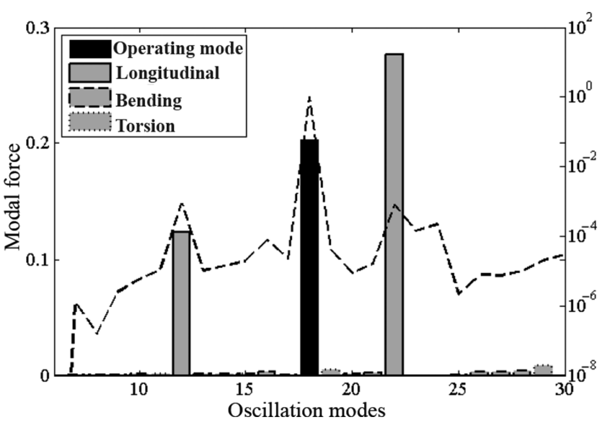

Figure 8: Modal force and modal amplitude at operational frequency (dashed line) for a radial mounting force.

In Figure 8 the calculated results in case of radial fixation exclusively (cf. Figure 7, left) are illustrated. With the results showing that the applied radial forces have a strong effect on longitudinal modes and especially the operational mode, the conclusion can be drawn that the mounting should be soft in radial direction. Reversely, normal mounting forces in z-direction at the same position on the transducer have no impact on the operational mode (cf. Figure 9) because the mounting is located near a respective oscillation node.

In addition, the harmonic solution of the model is given in Figure 9 (dotted line). Here the harmonic

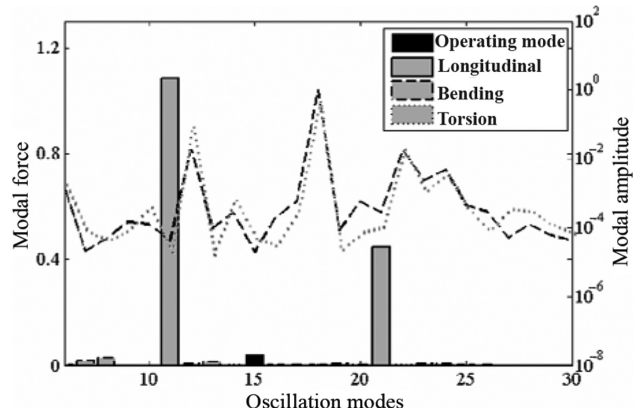

Figure 9: Modal force and modal amplitude (dashed line) as well as the result of non-reduced model (dotted line) at operational frequency for mounting force in z-direction.

solution is calculated directly and then transferred to the modal space allowing comparison with the results of the analysis method described in the contribution at hand. Considering the significantly reduced calculation time (more than 99% reduction) a sufficient degree of conformance is achieved.

Nevertheless, it becomes apparent that various investigations concerning the mounting of ultrasonic transducers are possible and relatively easy to perform by means of the analysis method at hand.

Conclusion

A modal transformation-based analysis method for investigating load influences on transducer vibration in ultrasonic-assisted machining has been developed and presented. A special focus here was on the excitation of eigenmodes and the respective impact on the operational vibration. It has been shown that determining the individual oscillation modes being excited by certain loads is possible by means of a defined modal force. Determining, in addition, the defined modal amplitude allows evaluation of the qualitative impact of the respective eigenmodes on the transducer vibration at a certain frequency and node. Both modal parameters and the complete analysis method, respectively, are presented by means of an explicit example. In this regard process loads as well as mounting loads have been investigated. With the developed method permitting various conclusions for each particular eigenmode in dependence of the different load setups a versatile usable instrument for investigating load influences on ultrasonic transducers has been created. In addition the entire method is distinguished by its efficiency that is caused by carrying out the analysis on the modal transformation results directly.

Funding: The work was supported by the German Research Foundation (DFG).

References

Babitsky, V. I., A. N. Kalashnikov, A. Meadows, and A. A. H. P. Wijesundara. 2003. "Ultrasonically Assisted Turning of Aviation Materials." *Journal of Materials Processing Technology* 132:157–67.

Crispi, F. J., G. C. Maling, and A. W. Rzant. 1972. "Monitoring Microinch Displacements in Ultrasonic Welding Equipment." *IBM Journal of Research and Development* 16 (3):307–12.

Heisel, U., R. Eber, G. Wolf, J. Wallaschek, J. Twiefel, and M. Huang. 2011. "Investigations on Ultrasonic-Assisted Drilling and Milling of Stone." In 1st International Conference on Stone and Concrete Machining, 117–22, Hanover, November 23–24.

Heisel, U., R. Eisseler, R. Eber, J. Wallaschek, J. Twiefel, and M. Huang. 2011. "Ultrasonic-Assisted Machining of Stone." *Production Engineering* 5 (6):587–94.

Littmann, W., H. Storck, and J. Wallaschek. 2001. "Sliding Friction in the Presence of Ultrasonic Oscillations." *Archive of Applied Mechanics* 71:549–54.

Rozenberg, L. D. 1969. *Sources of High-Intensity Ultrasound*. Vol. 1, 216. New York: Plenum Press.

Rozenberg, L. D., V. F. Kazantsev, L. O. Makarov, and D. F. Yakhimovich. 1964. *Ultrasonic Cutting*. New York: Consultants Bureau.

Weaver, V., S. P. Timoshenko, and D. H. Young. 1990. *Vibration Problems in Engineering*, 5th ed. Fong and Sens Printers Ltd. New York: J. Wiley & Sons.

Zhang, H., F. Wang, Y. Tian, X. Zhao, D. Zhang, and L. Han. 2013. "Electrical Matching of Low Power Piezoelectric Ultrasonic Transducers for Microelectronic Bonding." *Sensors and Actuators A: Physical* 199:241–9.